Pflügers Arch – Eur J Physiol (1995) 429:738–747

ORIGINAL ARTICLE

H. Lerche · Ch. Fahlke · P.A. Iaizzo
F. Lehmann-Horn

Characterization of the high-conductance Ca^{2+}-activated K^+ channel in adult human skeletal muscle

Received: 31 May 1994/Received after revision: 22 August 1994/Accepted: 13 September 1994

Abstract Ca^{2+}-activated K^+ channels of a large conductance (BK_{Ca}) in human skeletal muscle were studied by patch clamping membrane blebs and by using the three microelectrode voltage-clamp recording technique on resealed fibre segments. Single-channel recordings in bleb-attached and inside-out modes revealed BK_{Ca} conductances of 230 pS for symmetrical and 130 pS for physiological K^+ distributions. Open probability increased with membrane depolarization and increasing internal $[Ca^{2+}]$. The Hill coefficient was 2.0, indicating that at least two Ca^{2+} ions are required for full activation. Kinetic analysis revealed at least two open and three closed states. An additional long-lived inactivated state, lasting about 0.5–20 s, was observed following large depolarizations, when extracellular K^+ was lowered to physiological values. BK_{Ca} were blocked by three means: (1) externally by tetraethylammonium which reduced single-channel amplitude (IC_{50} approx. 0.3 mM); (2) internally by polymyxin B which decreased the open probability (IC_{50} approx. 5 μg/ml); and (3) externally by charybdotoxin which caused long-lasting periods of inactivation ($IC_{50} < 10$ nM). Measurements on resealed fibre segments at physiological $[K^+]$ were in accordance with the single-channel data: only when intracellular $[Ca^{2+}]$ was elevated did charybdotoxin (50 nM) reduce the macroscopic membrane K^+ conductance with depolarizing voltage steps.

H. Lerche · P.A. Iaizzo[1] · F. Lehmann-Horn (✉)
Department of Applied Physiology, University of Ulm, D-89069 Ulm, Germany

Ch. Fahlke
Department of General Physiology, University of Ulm, D-89069 Ulm, Germany

Permanent address:
[1]Departments of Anesthesiology and Physiology, University of Minnesota, 420 Delaware Street SE, Minneapolis, MN 55455, USA

Key words Adult human skeletal muscle
Ca^{2+}-activated K^+ channels · Patch clamp
Sarcolemmal blebs · Resealed fibre segments
Caffeine · Fura-2 · Intra-bleb ionic composition

Introduction

Ca^{2+}-activated K^+ channels are found in most excitable and non-excitable tissues [4]. They are classified into small (SK_{Ca}), intermediate (IK_{Ca}) and large (BK_{Ca}) populations according to their conductance. The apamin-sensitive SK_{Ca} are present in cultured muscle cells [3] and in muscles from patients with myotonic dystrophy [27]. In adult skeletal muscle only BK_{Ca} are found. They are specifically blocked by charybdotoxin (CTX) [23], a venom component of the scorpion *Leiurus quinquestriatus* (for reviews see [3, 12]).

The aim of this study was to characterize BK_{Ca} in native adult human skeletal muscle. To do so, characteristics of single channels were determined and compared to results obtained using a three microelectrode voltage-clamp technique.

Materials and methods

Muscle biopsies

Human muscle specimens were obtained from individuals who had undergone a muscle biopsy for the exclusion of susceptibility to malignant hyperthermia. Only muscle from patients with a negative test result was subsequently used for patch-clamp or intracellular measurements. Fibre segments about 3 cm long and 0.5 cm in diameter were removed from the quadriceps femoris under regional anaesthesia and were divided further into bundles with diameters of 2–3 mm. All procedures were in accordance with the Helsinki convention and were approved by the Ethics Commission of the Technical University of Ulm.

Patch-clamp recordings

Sarcolemmal blebs were formed mechanically without any enzymatic treatment [28]. Briefly, a muscle bundle was placed in a relaxing 130 mM K^+ methane sulphonate (KMeS) solution in a sylgard-based preparation chamber (in mM): KMeS 130, $MgCl_2$ 2, ethylenebis(oxonitrilo) tetraacetate (EGTA) 2, 4-(2-hydroxyethyl)-1-piperazineethanesulphonic acid (HEPES) 5, pH 7.2 (= preparation solution). When stored in this solution at 4 °C, the muscle was viable for study for 48 h. Segments of single fibre, about 1 cm in length, were removed under microscopic observation (10x) using fine forceps. Next, the segments were pinned at both ends to the bottom of a plastic Petri dish which served as the recording chamber. When the bathing solution contained more than 10^{-5} M Ca^{2+} the fibre segments contracted and immediately numerous sarcolemmal blebs (10–100 per fibre) were formed; they also appeared at lower $[Ca^{2+}]$ but to a much lesser extent [15].

Selected free $[Ca^{2+}]$ values were obtained by adding various amounts of $CaCl_2$ to the preparation solution according to Fabiato [8]. For a $[Ca^{2+}]$ greater than 10^{-5} M, EGTA was omitted and $CaCl_2$ added as necessary. Localized solution exchange at the internal side of the sarcolemma in inside-out patches was achieved with a liquid filament. The patch pipette contained the preparation solution for a symmetrical K^+ distribution, or the following solution composition for a physiological K^+ distribution (in mM) : NaMeS 120, KMeS 3.5, $CaCl_2$ 1, Na_2HPO_4 0.67, NaH_2PO_4 0.22, HEPES 15, pH 7.4.

In some cases the following agents were added to either solution: tetraethylammonium chloride (TEACl), polymyxin B (both Sigma, Deisenhofen, Germany) or CTX (Latoxan, Rosance, France).

Pipettes of borosilicate glass were drawn with a three-step puller (Zeitz, Augsburg, Germany), sylgard coated and firepolished to a final resistance of 5–7 MΩ. Seals of about 10 GΩ were regularly obtained. The patches commonly contained one to three channels, and in a few rare cases, more than five. Primarily, recordings were obtained in the bleb-attached or inside-out modes. It was not possible to routinely establish the "whole-bleb" configuration to obtain outside-out patches [9]. However, outside-out patches sometimes appeared spontaneously, probably due to rupture of the inner membrane of a closed mini-vesicle at the tip of the pipette: they were recognized by an inverse relationship between open probability (P_{open}) and voltage, and some of them were stable enough for recordings.

Data were recorded by means of an EPC7 amplifier (List, Darmstadt, Germany), stored on a modified DAT recorder (48 kHz digitization rate, Sony) and evaluated off-line. They were low-pass filtered at 3 kHz (–3 dB) with an analogue eight-pole Bessel filter (Zeitz), digitized at a rate of 10 kHz and analysed with a personal computer using p-Clamp (Axon Instruments, Foster City, Calif., USA) and in house software. To determine the time constants of dwell-time distributions, original recordings lasting 30 s were idealized using a 50 % amplitude criterion. Semilogarithmic plots of all events were fitted by least-squares analysis (p-Clamp, version 5.5.1) using one to four exponential functions [6]. Only patches containing a single channel were evaluated, as was concluded when only a single open level was seen at a high P_{open} value (≥ 0.8) and over the whole recording period of at least 5 min. Closed states which exceeded by six times the longest closed time constant were designated as long-lived closed states.

Intra-bleb fura-2 trapping

To evaluate the content of the intra-bleb milieu, it was determined whether or not the membrane-impermeable form of fura-2 (mol. wt. = 832 g) entered the blebs during their formation (see Results). The bleb preparation was performed in a solution containing (in mM): KMeS 130, $MgCl_2$ 2, $CaCl_2$ 1, HEPES 5, pH 7.2 and 25 μM of the pentapotassium salt of fura-2 (= fura solution). According to the dissociation constant of fura-2 (i.e. K_d = 240 nM), in this solution fura-2 was saturated by Ca^{2+} ions. Fura-2 fluorescence intensities were measured with a photomultiplier which was attached to a microscope photometer adapted for wavelengths 340/380 nm (PM 200, Zeiss, Germany). The measuring field was restricted to the bleb area: 10×10 μm^2 to 25×25 μm^2. The absolute intensity values were normalized to the free fura-2 intensity using Sigma plot 5.0 (Jandel Scientific, Erkrath, Germany).

Three electrode voltage-clamp

The voltage-clamp set-up and the experimental protocol were as described previously [14], but data collection and data analysis were simplified by the use of an AT personal computer system in combination with an AD converter (Burr-Brown, PCI 2000) and in house software.

Briefly, for the determination of the steady-state relationship between membrane current density and membrane potential, resealed fibre segments [13] were impaled midway along their length with three capacity-compensated microelectrodes. All measurements were performed at 37°C in a Cl^--free solution of the following composition (in mM) : NaMeS 108, KMeS 3.5, Ca^{2+} gluconate 1.5, $MgSO_4$ 0.7, $NaHCO_3$ 26.2, NaH_2PO_4 1.7, Na^+ gluconate 9.6, 315 mosmol/l. The pH was adjusted to 7.4 by gassing the solutions with a mixture of 95 % O_2 and 5 % CO_2. All solutions contained 1 μM tetradotoxin (TTX, Roth, Karlsruhe, Germany), some of them caffeine (Merck, Darmstadt, Germany) and/or CTX. In order to suppress unspecific binding of CTX to the recording chamber (or to the patch-pipette wall), 0.05 % albumin was added to the solution.

Results

Intra-bleb ionic composition and fura-2 trapping

Single-channel recordings were performed on mechanically formed sarcolemmal blebs. Bleb-attached patches were obtained more readily and were more stable than those obtained in the inside-out mode. However, there is concern as to the ionic composition of the intra-bleb solution. Interestingly, we observed that P_{open} remained stable when membrane patches were transferred from the bleb-attached to the inside-out configuration. This observation indicated that the bleb-filling solution contained the same amount of free Ca^{2+} as the bathing solution. This conclusion was supported by the similar P_o values for five bleb-attached and five inside-out patches at pCa 6 (Fig. 1A), where pCa is equal to $-\log_{10}[Ca^{2+}]$.

To test if components of the bathing solution could enter the blebs via non-channel-mediated mechanisms, we determined the intra-bleb concentration of a large, membrane-impermeable molecule (fura-2) added to the bathing solution prior to bleb formation (see Materials and methods). In Fig. 1B (I), the Ca^{2+}-bound fura-2 fluorescence intensity is shown before washing. As fura-2 was saturated by Ca^{2+} ions (see Materials and methods), the free fura-2 fluorescence had the same intensity as the background. When fura-2 was washed out from the bathing solution, there was a significantly

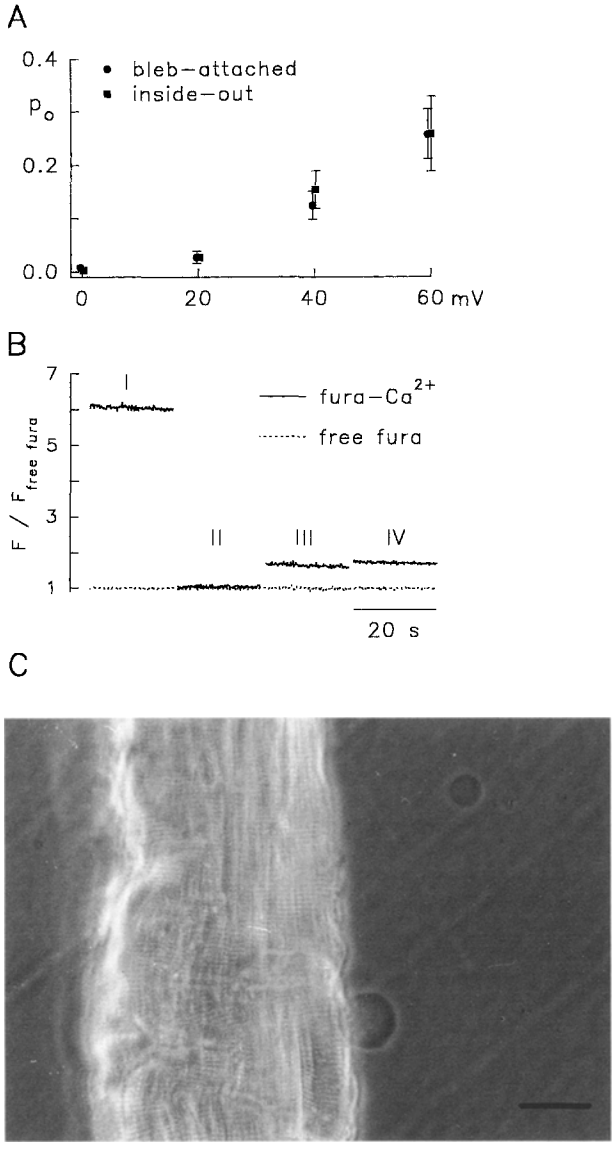

Fig. 1A–C Determination of the intra-bleb milieu. **A** Comparison of the open probability (P_{open}) of 5 bleb-attached and 5 inside-out patches. The Ca^{2+} concentration of the bathing solution was 10^{-6} M. The pipette solution contained 3.5 mM K^+. There was no statistical difference in P_{open} at any potential between these two patch modes. **B** Fluorescence intensities (F) of Ca^{2+}-bound fura-2 (excitation at 340 nm) and of free fura-2 (380 nm), normalized to the free fura-2 intensity ($F_{free\ fura}$). 4 *Trace I*: F of a 2-mm fluid column of a solution containing 25 μM fura-2 and 1 mM Ca^{2+} (before washing); *trace II*: the lack of background F following washout of fura-2; *Traces III, IV*: F of two detached blebs (like the *upper bleb* shown in **C**) following washout of fura-2. The results suggest that fura-2 entered the blebs during their formation and remained within. **C** Shown is a muscle fibre with an attached and a detached sarcolemmal bleb. The *bar* represents 25 μm

higher Ca^{2+}-bound fura-2 fluorescence signal associated with blebs which had detached from the fibre Fig. 1B (III, IV) than was associated with the background [Fig. 1B (II); a detached bleb is shown in Fig. 1C]. This fluorescence was also visible through the microscope. Thus, the membrane-impermeable fura-2 was trapped in these detached blebs. Because the blebs have a diameter of only 10–25 μm, the fluorescence intensity of Ca^{2+}-bound fura-2 after washing (III, IV) was much less than the fluorescence intensity of the fluid column of 2 mm of optical depth before washing (I). Moreover, the fluorescence intensity decreased over time presumably due to photobleaching, as observed by the small decrease in intensity over the measuring time of 20 s (I, III and IV).

Single-channel recordings

BK_{Ca} in membrane blebs of human skeletal muscle were active in the whole investigated potential range of − 60 mV to + 60 mV. At a constant internal [Ca^{2+}] the percentage of time the channels spent in the open state increased with membrane depolarization (Fig. 2A–C). In the symmetrical 130 mM K^+ solution, BK_{Ca} were slightly inwardly rectifying and had a conductance of 230 pS in the voltage range of between −60 mV and + 15 mV. In a physiological K^+ distribution, and for two outside-out patches with the designed extracellular solution at the cytoplasmic side of the membrane (see Materials and methods), the conductance was 130 pS at 0 mV. No Na^+ blockage of BK_{Ca} occurred in the outside-out mode, although the pipette solution contained 120 mM Na^+. This was attributed to the high K^+ concentration in the bathing solution, as external K^+ ions were found to antagonize the Na^+ blockage [20].

Ca^{2+} and voltage dependence

The P_{open} of the BK_{Ca} was dependent on both the internal [Ca^{2+}] and the clamp potential (Fig. 3C). In Fig. 3A, current recordings from a patch containing at least seven BK_{Ca} shows activation and deactivation at constant voltage by the internal application of solutions with a pCa of 5 or 7 respectively. As illustrated in Figs. 3B, C and 4C, this is a similar range of internal [Ca^{2+}] values at which the channel was either maximally gated or closed. The Hill coefficients for the Ca^{2+}-binding reaction, derived from the Hill plots shown in Fig. 3D, were all close to 2, indicating that at least two Ca^{2+} ions are required for full channel activation.

Long-lasting periods of inactivation, also called long-lived closed states by Malebran et al. [18], seldom occurred in symmetrical K^+ solutions (see Fig. 8A,B), but became prominent when external K^+ was lowered to physiological values, as shown in Fig. 4A. The probability of the channel not being in a long-lived closed state was defined as P_{active}, the open probability during the active state as P_{open} (Fig. 3) and the product of these as P_{total} (Fig. 4B). P_{total} was determined by measurements lasting about 1 min (upper traces in Fig. 4A),

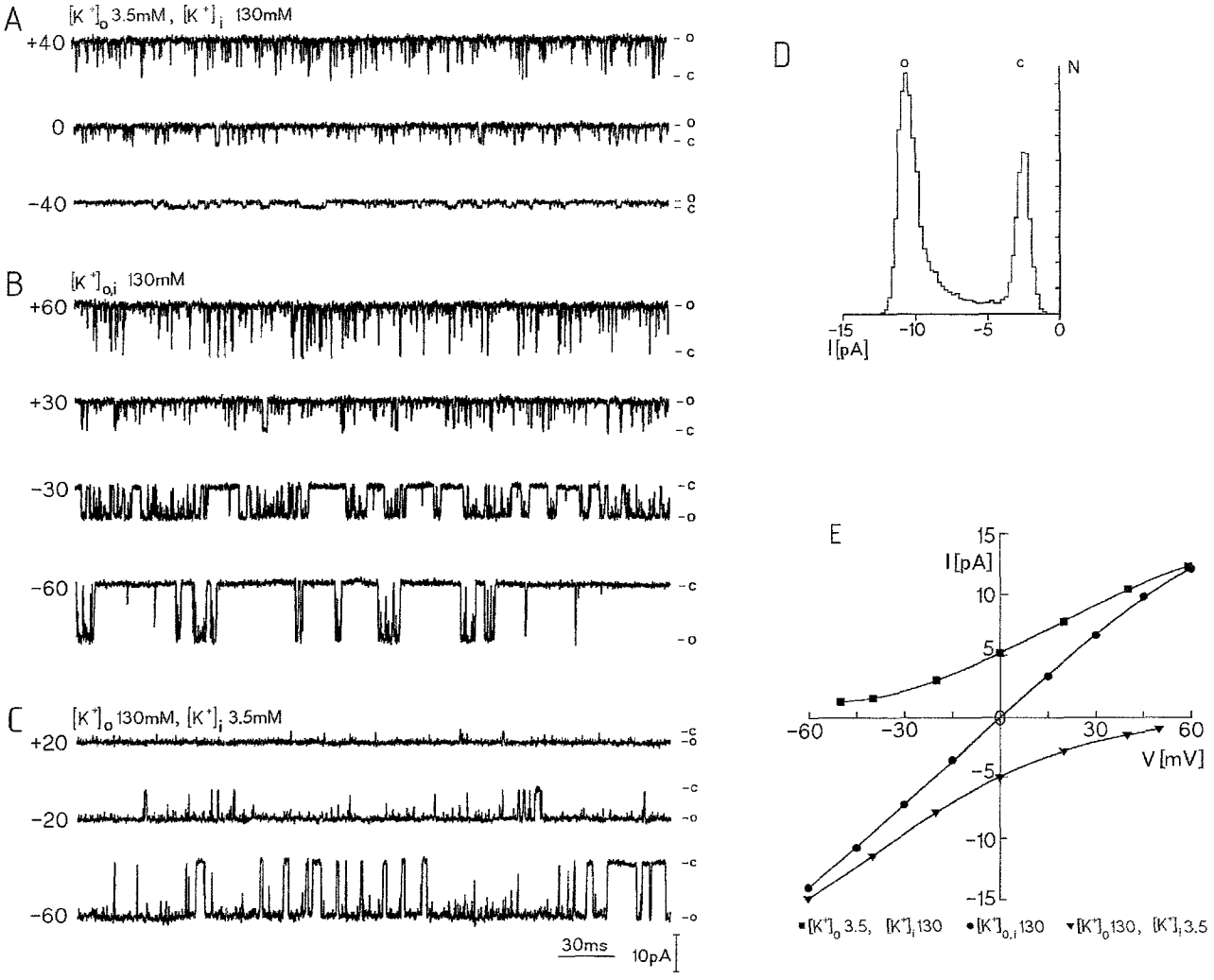

Fig. 2A–E Current/voltage relationship of a single large-conductance, Ca^{2+}-activated K^+ channel (BK_{Ca}). **A–C** Original recordings at different membrane potentials; external ($[K^+]_0$) and internal ($[K^+]_i$) K^+ concentrations are indicated in mM. **D** Amplitude histogram of all sampling points of *trace* 3 in B. **E** Current/voltage relationship at different $[K^+]$ values. Data points of the *upper* and *middle curves* were averaged from 12 inside-out or bleb-attached patches, whereas the *lower curve* was from 2 outside-out patches. Shown are means ± SEM (which were mostly smaller than *symbol size*); curves are fitted with four polynomials

P_{open} by excluding the long-lived inactivated state from the analysis (lower traces in 4A), and P_{active} was calculated as P_{total}/P_{open}. P_{active} had an inverse voltage dependence in comparison to P_{open} so that P_{total} decreased at both hyperpolarizing and depolarizing clamp potentials (Fig. 4B). This yielded a unique distribution of the open probabilities for physiological $[K^+]$ (Fig. 4C) than those for symmetrical $[K^+]$ (Fig. 3C).

Dwell time distributions

Figure 5 shows the dwell time evaluation from a patch containing one single BK_{Ca} that was stable long enough for a study at three pCa values, i.e 7, 6 and 5, over the whole voltage range between –60 mV and + 60 mV. The open time distribution was described by a second-order exponential (Fig. 5A), whereas the closed time distribution was best fitted by a third order (Fig. 5C). Examples of short, intermediate and long opening or closing events are illustrated by the traces in Fig.5A and C. As previously described by Magleby and Palotta [17], the different closed states were designated as flickers (short events) or gaps within bursts (intermediate events) and gaps between bursts (long events).

Seven patches in which only one channel was identified showed qualitatively the same results. In general, the open and shut components with maximum mean lifetimes were dependent on both the internal $[Ca^{2+}]$ and the clamp potential and thus, on P_{open}, whereas the other components were not (Fig. 5B, D). The

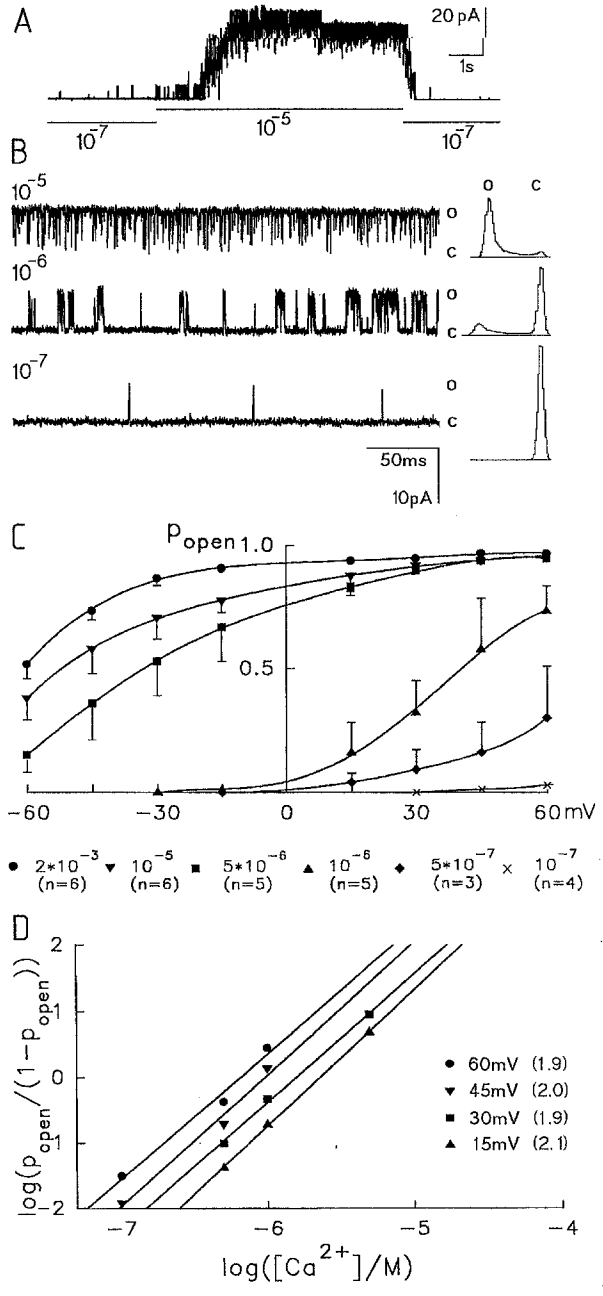

Fig. 3A–D P_{open} of BK_{Ca} was both $[Ca^{2+}]$ and voltage dependent. **A** Activation and block of BK_{Ca} in an inside-out patch containing 7 channels by changing pCa from 7 to 5 and back to 7; clamp potential = 0 mV, physiological $[K^+]$. **B** Representative recordings from 2 inside-out patches at the indicated $[Ca^{2+}]$; to the *right* are amplitude histograms summarizing 30 s of continuous recording; clamp potential = 30 mV, symmetrical $[K^+]$. **C** Dependence of P_{open} on $[Ca^{2+}]$ (indicated on the *bottom line*) and voltage at symmetrical $[K^+]$; data are pooled from bleb-attached and inside-out patches; curves are fitted with 2–4 polynomials. **D** Hill plot of mean values in **C** at positive potentials. The calculated Hill coefficients are indicated in *parentheses*

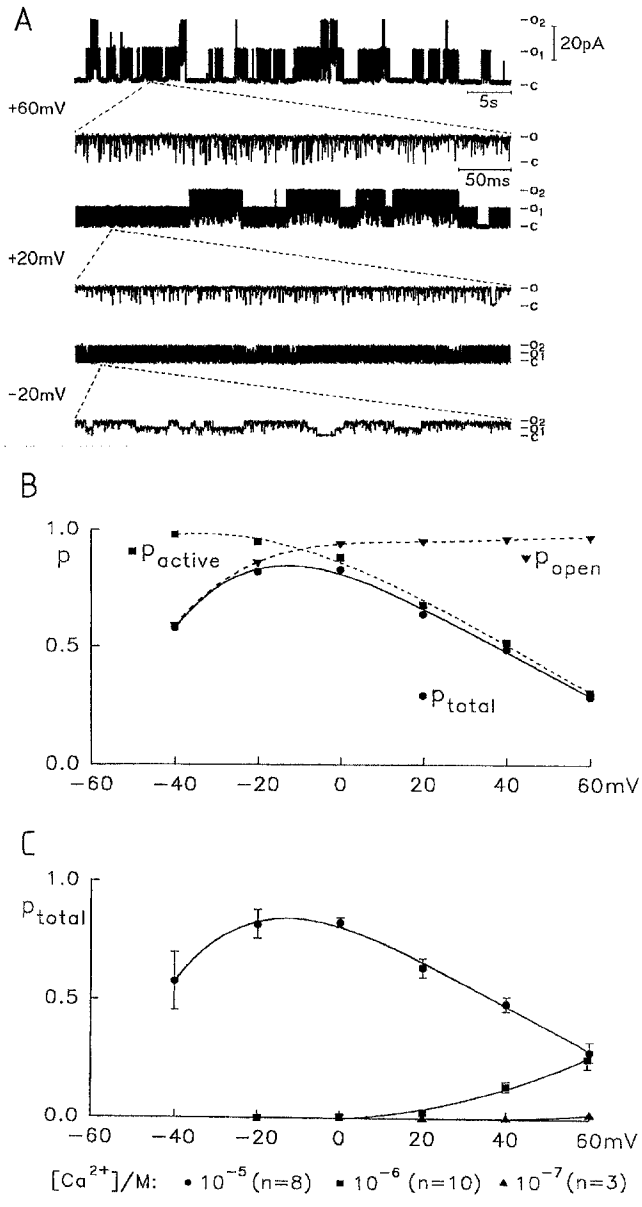

Fig. 4A–C Long-lived inactivated state at physiological $[K^+]$. **A** Recordings of a representative patch containing two BK_{Ca}. The *upper traces* demonstrate the probability of being in the active state (P_{active}, closures correspond to long-lived inactivations), and the *lower traces* are sections from the *upper traces* at a higher time resolution to show P_{open} during the active state. **B** The curves of P_{open}, P_{active} and the product of both, P_{total}, are fitted with 2–4 polynomials; pCa = 5; $n = 8$ bleb-attached or inside-out patches. **C** Dependence of P_{total} on $[Ca^{2+}]$ and voltage

percentage of short, intermediate and long events in relation to the total number of events varied with P_{open}: at pCa 7 (P_{open} approximates 0.05) the percentage of short open events was greater than or equal to 0.5, whereas at pCa 5 ($P_{open} > 0.9$) the short component was negligible. At a P_{open} greater than or equal to 0.9, gaps between bursts were extremely rare, and within bursts the ratios of gaps/flickers ranged between 0.05/0.95 and 0.3/0.7. At a P_{open} of 0.1, the percentage of gaps between bursts was greater than or equal to 0.5, and within bursts the ratios of gaps/flickers remained in the same range as at a high P_{open}.

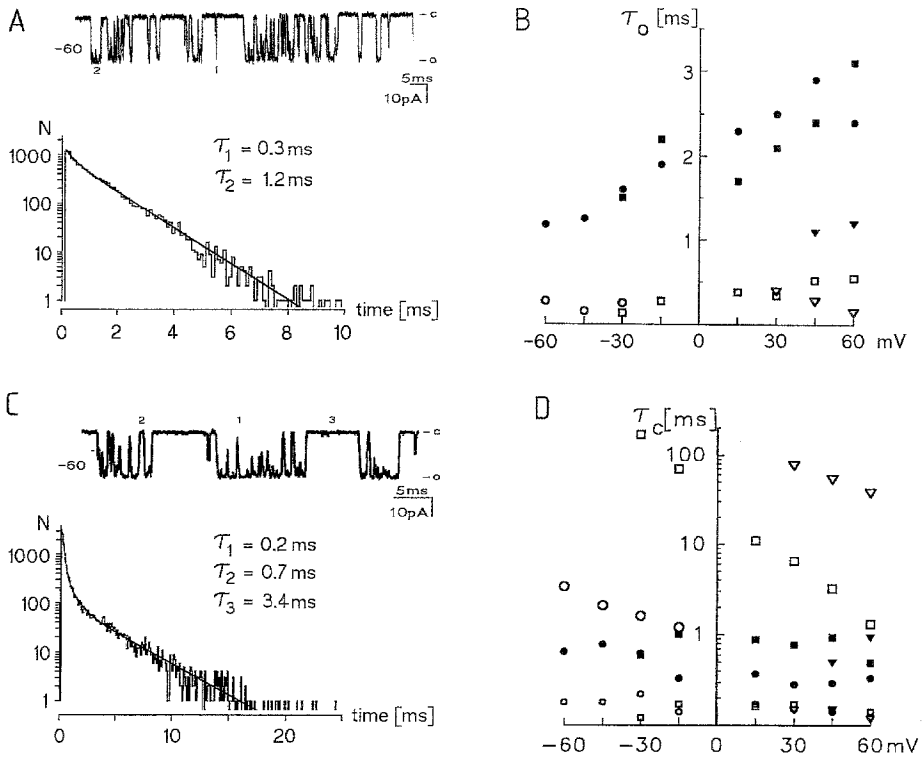

Fig. 5A–D Dwell time distributions of BK_{Ca}. **A, C** Semilogarithmic plots of open (**A**) and closed (**C**) events during 30 s of continuous recording at − 60 mV, pCa 5. The *lines* are fits with 2 and 3 exponentials, respectively. The *numbers* above the *traces* mark typical events of each exponential component. **B, D** Dependence on $[Ca^{2+}]$ and voltage of all open (**B**) and closed (**D**) exponential components. *Circles* = pCa 5, *squares* = pCa 6, *triangles* = pCa 7. **B** *Filled symbols* denote long components and *open symbols* short components. **D** *Large open symbols* denote long components, *filled symbols* intermediate components and *small open symbols* short components. All data are derived from the same first bleb-attached (pCa 5) and subsequently inside-out (pCa 6 and 7), patch containing only a single channel

Pharmacological aspects

To provide the most stable P_{open} over a large potential range we chose a high internal $[Ca^{2+}]$ of 2 mM for the pharmacological experiments. The rapid, complete and reversible block of 5 mM TEA when applied externally is shown in Fig. 6A for an outside-out patch containing five BK_{Ca} channels. Because it was not possible to routinely establish outside-out patches (see Materials and methods), TEA was added to the pipette solution. TEA evoked a very fast block [10] of BK_{Ca}, which resulted in an apparent reduction of the single-channel amplitude (Fig. 6B). With 0.1 mM TEA added to the pipette solution, the single-channel conductance was 140 pS and with 1 mM TEA it was 43 pS (control 230 pS, Fig. 6C), thus yielding an estimated IC_{50} of 0.3 mM; P_{open} or P_{active} were not affected. The data are in accordance with the TEA-induced reduction of the single-channel conductance in a wide variety of K^+ channels [7].

Polymyxin B, a peptide antibiotic and inhibitor of protein kinase C ([30] and references therein), blocked the channel internally by decreasing P_{open} (an intermediate block as described by Hille [10]). Figure 7A shows recordings under control conditions and during application of 5 μg/ml and 50 μg/ml polymyxin B from one single inside-out patch containing four BK_{Ca}. P_{open} in the presence and absence of polymyxin B was determined from recordings lasting 30 s at each voltage. The polymyxin B block was voltage dependent, being more effective at more positive clamp potentials. For example, at zero potential, polymyxin B (5 μg/ml) blocked about 50 % of the channel activity, and application of 50 μg/ml polymyxin B resulted in nearly a complete block (Fig. 7B); the channel conductance and P_{active} were unaffected. It took approximately 1 min until the block was fully established and polymyxin B was a difficult agent to wash out; e.g. in one patch, 50 μg/ml polymyxin B reduced P_{open} from 0.9 to 0.01, and 20 min after attempts to wash it out, the P_{open} was still 0.4 (not shown).

The effects of CTX on the BK_{Ca} revealed a slow blocking mechanism [10]; i.e. this scorpion toxin introduced long periods of quiescence (Fig. 8A) that were indistinguishable from the long-lived inactivated state described above (Figs. 4, 8A, C). To determine P_{active}, activity was recorded for at least 3 min and up to 7 min at each voltage. CTX was added directly to pipette solution because it has been described previously to be effective only when applied externally [1]. The cessation of BK_{Ca} activity was more prominent at hyperpolarizing voltages which was in contrast to the blocking effects of polymyxin B. A CTX concentration of 50 nM was highly effective and the IC_{50} was less than 10 nM, as shown in Fig. 8B; the channel conductance and P_{open} were not affected.

Because P_{active} decreased strongly with increasing depolarization in the presence of physiological $[K^+]$ (see Fig. 4) and because of the voltage dependence of the CTX block, it was verified that a concentration of 50 nM CTX produced a significant block with a physiological $[K^+]$ at an internal $[Ca^{2+}]$ of 10^{-5} M.

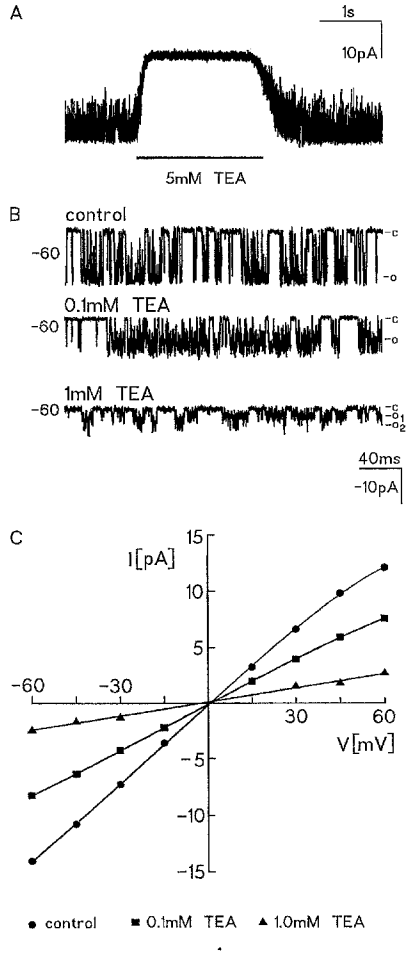

Fig. 6A–C Effects of tetraethylammonium (TEA) on BK_{Ca} activity. **A** Reversible block of 5 channels with 5 mM TEA in an outside-out patch. Pipette solution: 3.5 mM K^+, 1 mM Ca^{2+}. External solution: 130 mM K^+; clamp potential 0 mV. **B** Reduction of single-channel amplitude with either 0.1 mM or 1 mM TEA added to the pipette solution, in symmetrical 130 mM K^+ and at an internal $[Ca^{2+}]$ of 2 mM. The first two recordings are derived from patches containing a single channel, the third is from a patch with two channels (*bottom trace*). **C** A decrease in the single-channel conductance to 140 pS with 0.1 mM external TEA and to 43 pS with 1 mM TEA (control 230 pS, same curve as in Fig.2E). Both curves are derived from mean values from two bleb-attached patches each

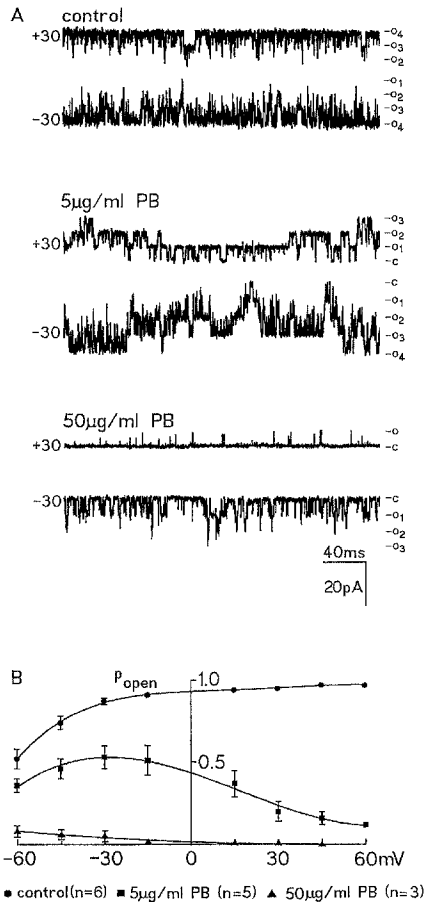

Fig. 7A, B The effects of polymyxin B on BK_{Ca} activity. **A** All traces are derived from the same, bleb-attached (control) and subsequently inside-out (polymyxin B applications) patch containing 4 channels. Polymyxin B was applied from the internal side; symmetrical 130 mM K^+; internal $[Ca^{2+}] = 2$ mM. **B** Voltage dependence of the polymyxin B block at concentrations of 5 μg/ml and 50 μg/ml (*PB*). Indicated are means ± SEM and the numbers of patches in *parentheses*; curves are fitted with 2–4 polynomials

The results from five control patches and three patches with CTX (containing 1, 4 and 5 channels) showed that a significant block occurred at physiologically relevant voltages up to 20 mV (Fig. 8C, D).

Three microelectrode voltage-clamp

In order to characterize the macroscopic Ca^{2+}-activated K^+ conductance, the steady-state K^+ conductance was measured at resting and elevated intracellular $[Ca^{2+}]$ in the presence and absence of CTX. The recordings were performed on resealed fibre segments [13] with the three microelectrode voltage-clamp technique in Cl^--free bathing solution containing 1 μM TTX, thus the Cl^- and Na^+ conductances were negligible. Intracellular $[Ca^{2+}]$ was elevated by adding 25 mM caffeine to the bathing solution which regularly induced contractures. Average resting potentials were between − 70 mV and − 80 mV in all solutions, i.e. they were not significantly altered by the addition of caffeine and/or CTX; the holding potential was adjusted to − 80 mV. CTX and caffeine, when separately added to the bathing solution, did not markedly alter the K^+ conductance at resting intracellular $[Ca^{2+}]$. In contrast, when intracellular $[Ca^{2+}]$ was increased by administering caffeine, 50 nM CTX blocked a K^+ conductance at depolarizing voltage steps more positive than − 50 mV (Fig. 9).

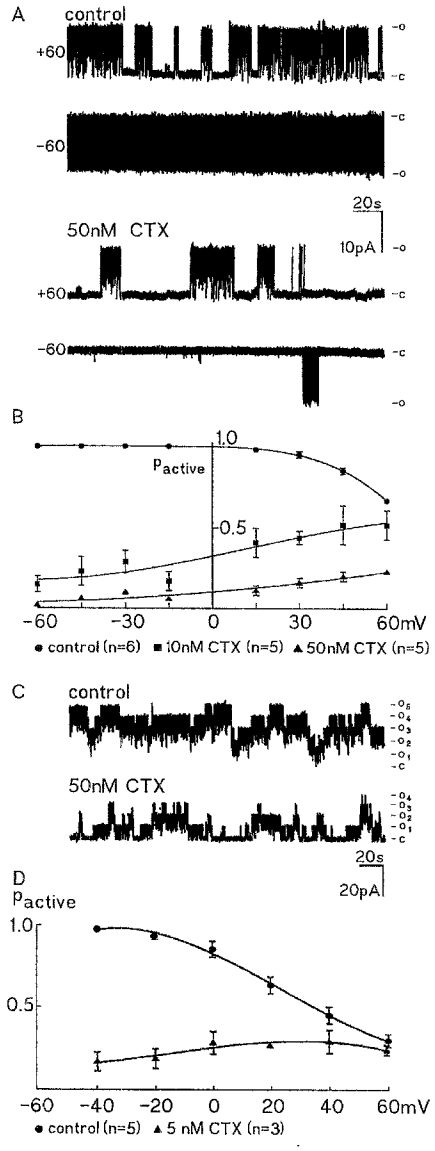

Fig. 8A–D Effects of charybdotoxin (CTX) on BK_{Ca} activity. **A** Recordings from 2 bleb-attached patches containing a single channel. CTX was added to the pipette solution (*lower two traces*). The $[K^+]$ was symmetrical at 130 mM, and internal $[Ca^{2+}]$ was 2 mM. **B** Voltage dependence of CTX block. Shown are means ± SEM; numbers of bleb-attached patches are given in *parentheses*; curves are polynomial fits. **C, D** Verification of CTX block with a physiological $[K^+]$ distribution and an internal $[Ca^{2+}]$ of 10^{-5} M. The original recordings are from 2 patches containing 5 channels each, both at 0 mV clamp potential. The *lower curve* in **D** is derived from 3 bleb-attached patches containing 1, 4 and 5 channels respectively. Shown are means ± SEM; curves are fitted with 2–4 polynomials

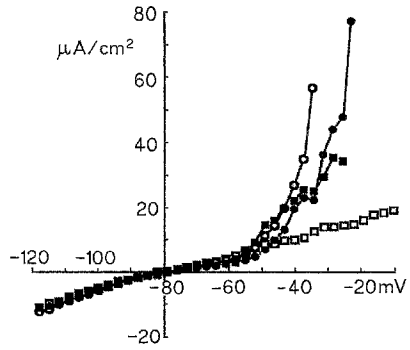

Fig. 9 The effects of CTX on the K^+ conductance measured in resealed fibre segments. The steady-state K^+ conductances were determined using three intracellular microelectrodes in a solution which was Cl^--free and contained 1 μM tetrodotoxin (TTX). (*Closed circles* control, average of $n = 29$ fibres, *open circles* plus 50 nM CTX, $n = 25$, *closed squares* plus 25 mM caffeine, $n = 16$, *open squares* plus 25 mM caffeine and 50 nM CTX, $n = 17$). The holding potential of all fibres was − 80 mV. At depolarizing voltage steps, the relationship determined for fibres bathed in a solution containing both caffeine and CTX was significantly different ($p < 0.05$; Student's *t*-test) from the other curves. Relationships for CTX and control solutions revealed no statistically significant differences because of the large standard deviations due to movement artefacts when the fibres were depolarized. In contrast, the fibres bathed in caffeine solution showed stable contractures and smaller standard deviation (not shown)

Discussion

Single-channel data

The single-channel conductance, the dependence on internal $[Ca^{2+}]$ and on voltage of BK_{Ca} described here are in agreement with previous results obtained from recordings of BK_{Ca} in non-human skeletal muscle [2, 11, 30] and of BK_{Ca} derived from mSlo, a mouse gene, expressed in *Xenopus* oocytes [5]. Previously reported Hill coefficients for mammalian BK_{Ca} were between 1.6 and 1.8 at positive voltages (i.e. those in rat muscle reconstituted in artificial lipid bilayers; [24]) whereas McManus and Magleby [22] reported a Hill coefficient of > 3.0, suggesting that the channel may bind up to four Ca^{2+} ions to become fully activated. In the present study, the calculated Hill coefficients were close to 2, which is close to the value in planar lipid bilayers. We do no know the reason for this difference, possible are developmental differences between embryonic and fully differentiated muscle, or the effects of a changed lipid composition [25] occurring during the bleb formation.

There have been several previous studies which have focused on the long-lived inactivated state of this channel. In one, Vergara and Latorre [29] showed evidence that these states are due to a blockage by a high internal $[Ca^{2+}]$, whereas Neyton and Miller [26] postulated that most of the Ca^{2+} blockage may be due to Ba^{2+} contamination. Subsequently, Malebran et al. [18, 19] verified the existence of a long-lived inactivated state at an internal $[Ba^{2+}]$ of 3 nM. The authors postulated that the long-lived inactivated state was not due to a Ba^{2+} or Ca^{2+} blockage and proposed a voltage-dependent gate. As also suggested by our results, all these studies indicated that the long-lived inactivated state increases with depolarization and with a decreasing external $[K^+]$.

Two open states and three (or four, if the long-lived inactivation state is included) different shut states would be predicted by our resultant dwell time analysis. Such behaviour has been determined also in a previous study of non-human tissue [17]. However, it should be noted that in a more detailed analysis of BK_{Ca} activity in cultured rat muscle, which used an increased frequency response and a larger number of events, McManus and Magleby [21] reported at least three open and six shut states for these channels.

It was previously reported that polymyxin B is most likely to exert its blocking effect at the Ca^{2+}-binding site of the channel protein [30]. Our results are not consistent with this hypothesis; according to which, polymyxin B should have shifted the current voltage dependence of P_{open} to positive potentials such as did low $[Ca^{2+}]$ (see Fig. 3C). In contrast to low $[Ca^{2+}]$, polymyxin B was most effective in blocking channels at positive potentials.

CTX was first described by Miller et al. [23] to block BK_{Ca} in rat skeletal muscle. Subsequently, both Anderson et al. [1] and MacKinnon and Miller [16] elucidated further the properties and mechanism of CTX block. They determined that the channel could be blocked either in the open or shut state, but that the association rate of CTX with the open channel was about sevenfold higher than with the closed channel, resulting in a more effective block at a higher P_{open}. Furthermore, in these studies at a constant P_{open}, the dissociation rate increased eightfold with a depolarization from -30 mV to 30 mV and the voltage dependence of the dissociation rate disappeared when internal K^+ was replaced by Na^+. Assuming that this occurs, the voltage dependence of CTX block in human skeletal muscle BK_{Ca} is predicted to be due to an increase of the dissociation rate upon depolarization: in our experiments, the internal $[K^+]$ was constantly high at 130 mM, and P_{open} relatively constant between 0.6 (-60 mV) and 0.95 (15–60 mV) (Fig. 2C).

In general, all single-channel data obtained from native human muscle preparations agree closely with earlier reported results from skeletal muscle in other species, which employed various methods.

Intra-bleb ionic composition

We have provided evidence that the $[Ca^{2+}]$ is the same in both the bathing and the bleb-filling solutions and that fura-2, a large molecule with a molecular mass of 832 g/mol, could enter sarcolemmal blebs. These findings, together with the recently reported absence of K^+ channel activity in belb-attached recordings with Cs^+ as the major cation in the bathing solution [15] indicate that the sarcolemma becomes unspecifically leaky during the formation of the blebs and thus allows an equilibration of the bathing solution with the intra-bleb milieu.

Bleb-attached recordings therefore allow definition of the ionic composition on both sides of the membrane without patch excision. Nevertheless, care should be taken in preparing blebs, for the presence or absence of intracellular components such as enzymes or peptides which could affect channel behaviour is unknown.

Three microelectrode voltage-clamp

Our intracellular recordings suggest that in human muscle fibres a CTX-sensitive Ca^{2+}-activated K^+ conductance at depolarizing voltage steps is negligible under resting conditions but becomes significant when intracellular $[Ca^{2+}]$ is elevated. A concentration of 50 nM CTX did not markedly influence the K^+ conductance under resting conditions. Hence, the delayed rectifier is not synonymous with the CTX-blocked conductance. On the other hand, certain aspects of the experiments, in which the intracellular $[Ca^{2+}]$ was increased by adding caffeine in the presence of CTX, are unclear. Assuming that caffeine activates the release of Ca^{2+} from the sarcoplasmic reticulum and, thus, the Ca^{2+}-activated K^+ conductance at depolarizing voltages without affecting other K^+ conductances, and assuming that the Ca^{2+}-activated K^+ conductance is selectively blocked by CTX, then the total K^+ conductance should be increased by addition of caffeine and should return to control values upon addition of CTX. In other words, at voltages more positive than -50 mV, the normal K^+ conductance and that in caffeine plus CTX should be the same, but it is not (the filled square curve in Fig. 9 should be positioned to the left of the three other curves, which themselves should not differ significantly. Plausible explanations for this unexpected result could be that there is a T-tubular swelling secondary to the caffeine-induced contracture which leads to the decrease in delayed rectifier K^+ conductance or to a direct action of either caffeine or Ca^{2+} on this conductance.

In summary, the BK_{Ca} channel in adult human skeletal muscle is chacterized by: (1) increasing activity with both internal $[Ca^{2+}]$ and depolarization; (2) the binding of at least two Ca^{2+} ions for full activation; (3) at least two open and three closed kinetic states; (4) a long-lived inactivated state occurring at low external $[K^+]$ following depolarization; and (5) block by external TEA, internal polymyxin B and external CTX.

Acknowledgements We want to thank Drs. H. Brinkmeier, C. Franke, S. Grissmer, A. Herrmann-Frank, K. Jurkat-Rott, S. Quasthoff and M. Schiebe for helpful discussions, Ms. U. Richter for technical assistance and Ms. S. Plate for secretarial help. The work was supported by the Deutsche Forschungsgemeinschaft (to F.L.H.). Paul A. Iaizzo was a visiting Professor of the Department of Applied Physiology.

References

1. Anderson CS, MacKinnon R, Smith C, Miller C (1988) Charybdotoxin block of single Ca^{2+}-activated K^+ channels: effects of channel gating, voltage, and ionic strength. J Gen Physiol 91:317–333
2. Barret JN, Magleby KL, Palotta BS (1982) Properties of single calcium-activated potassium channels in cultured rat muscle. J Physiol (Lond) 331:211–230
3. Blatz AL, Magleby KL (1986) Single apamin-blocked Ca^{2+}-activated K^+ channels of small conductance in cultured rat skeletal muscle. Nature 323:718–720
4. Blatz AL, Magleby KL (1987) Calcium-activated potassium channels. Trends Neurosci 10:463–467
5. Butler A, Tsonuda S, McCobb DP, Wei A, Salkoff L (1993) mSlo, a complex mouse gene encoding "maxi" calcium-activated potassium channels. Science 261:221–224
6. Colquhoun D, Sigworth FJ (1983) Fitting and statistical analysis of single channel records. In: Neher E, Sakman B (ed) Single-channel recording. Plenum, New York, pp 191–263
7. Cook NS, Quast U (1990) Potassium channel pharmacology. In: Cook NS (ed) Potassium channels: structure, classification, function and therapeutic potential. Ellis Horwood, Chichester pp 181–225
8. Fabiato A (1988) Computer programs for calculating total from specified free or free from specified total ionic concentrations in aqueous solutions containing multiple metals and ligands. Methods Enzymol 157:378–417
9. Hamill OP, Marty A, Neher E, Sakmann B, Sigworth FJ (1981) Improved patch-clamp technique for high-resolution current recording from cells and cell-free membrane patches. Pflügers Arch 391:85–100
10. Hille B (1992) Mechanisms of block. In: Hille B (ed) Ionic channels of excitable membranes. Sinauer Associates, Sunderland, Mass., pp 390–422
11. Latorre R, Vergara C, Hidalgo C (1982) Reconstitution in planar lipid bilayers of a Ca^{2+}-dependent K^+ channel from transverse tubule membranes isolated from rabbit skeletal muscle. Proc Natl Acad Sci USA 79:805–809
12. Latorre R, Oberhauser A, Labarca P, Alvarez O (1989) Varieties of calcium-activated potassium channels. Annu Rev Physiol 51:385–399
13. Lehmann-Horn F, Iaizzo P (1990) Resealed fibers segments for the study of the pathophysiology of human skeletal muscle. Muscle Nerve 13:222–231
14. Lehmann-Horn F, Rüdel R, Dengler R, Lorkovic H, Haass A, Ricker K (1981) Membrane defects in Paramyotonia congenita with and without myotonia in a warm environment. Muscle Nerve 4:396–406
15. Lerche H, Heine R, Pika U, George AL, Mitrovic N, Browatzki M, Weiss T, Rivet-Bastide M, Franke C, Lomonaco M, Ricker K, Lehmann-Horn F (1993) Human sodium channel myotonia: slowed channel inactivation due to substitutions for a glycine within the III-IV linker. J Physiol (Lond) 470:13–22
16. MacKinnon R, Miller C (1988) Mechanism of charybdotoxin block of the high-conductance, Ca^{2+}-activated K^+ channel. J Gen Physiol 91:335–349
17. Magleby KL, Palotta BS (1983) Calcium dependence of open and shut interval distributions from calcium-activated potassium channels in cultured rat muscle. J Physiol (Lond) 344:585–604
18. Malebran N, Latorre R, Cecchi X (1991) Calcium and long-lived closed states in a Ca^{2+}-activated K^+ channel from skeletal muscle (abstract). Biophys J 59:213
19. Malebran N, Latorre R, Cecchi X (1992) Large conductance calcium-activated K^+ channel gating is modulated by external cations (abstract). Biophys J 61:A14
20. Marty A (1983) Blocking of large unitary calcium-dependent potassium currents by internal sodium ions. Pflügers Arch 396:179–181
21. McManus OB, Magleby KL (1988) Kinetic states and modes of single large-conductance calcium-activated potassium channels in cultured rat skeletal muscle. J Physiol (Lond) 402: 79–120
22. McManus OB, Magleby KL (1991) Accounting for the Ca^{2+}-dependent kinetics of single large-conductance Ca^{2+}-activated K^+ channels in rat skeletal muscle. J Physiol (Lond) 443:739–777
23. Miller C, Moczydlowski E, Latorre R, Phillips M (1985) Charybdotoxin, a protein inhibitor of single Ca^{2+}-activated K^+ channels from mammalian skeletal muscle. Nature 313:316–318
24. Moczydlowski E, Latorre R (1983) Gating kinetics of Ca^{2+}-activated K^+ channels from rat muscle incorporated into planar lipid bilayers: evidence for two voltage-dependent Ca^{2+} binding reactions. J Gen Physiol 82:511–542
25. Moczydlowski E, Alvarez O, Vergara C, Latorre R (1985) Effect of phospholipid surface charge on the conductance and gating of a Ca^{2+}-activated K^+ channel in planar lipid bilayers. J Membr Biol 83:273–282
26. Neyton J, Miller C (1988) Potassium blocks barium permeation through a calcium-activated potassium channel. J Gen Physiol 92:549–568
27. Renaud JF, Desnuelle C, Schmid-Antomarchi H, Hugues M, Serratrice G, Lazdunski M (1986) Expression of apamin receptor in muscles of patients with myotonic muscular dystrophy. Nature 319:678–680
28. Quasthoff S, Franke C, Hatt H, Richter-Turtur M (1990) Two different types of potassium channels in human skeletal muscle activated by potassium channel openers. Neurosci Lett 119: 191–194
29. Vergara C, Latorre R (1983) Kinetics of Ca^{2+}-activated K^+ channels from rabbit muscle incorporated into planar bilayers:evidence for a Ca^{2+} and Ba^{2+} blockade. J Gen Physiol 82:543–568
30. Weik R, Lönnendonker U (1990) Polymyxin B as a highly effective gating modifier of high-conductance Ca^{2+}-activated K^+ channels in mouse skeletal muscle. Pflügers Arch 415: 671–677